5/19/2004

To: Thanh T. Nguyen, AU 2813, JEF-7D29

From : Jeff Harrison, STIC-EIC2800
JEF-4B68, 22511

Jeff

Re: 09/919,036
Specific mathematical expression for etch rate

Attached are the closest items I could find today. None are identical to the desired equation, but perhaps some of these are of use.

If you would like additional information, please contact me. Thanks.

-----Original Message-----
From: Nguyen, Thanh
Good Morning Jeff, would you please help me search for the above application especially the etching rate formula:
$ER(C,T) = ER_o \times C^{(-Ea/RT)} + A$
Or
$ER(C) = K \times C + A$
Where in ER is eth rate
K and A are first and second constants
C is the etching solution concentration
T is the solution temperature
Ea is the etching activation energy
R is gas constant

Thank you so much for your help,
Please let me know if you have any question,
thanh nguyen (2813)
272-1695

- A Remote Inspection System for Elevators

NEW PRODUCTS

- **The FPR-MKII Finger Print Recognize**

For complete PDF edition

Intelligent Transport Systems Edition
ISSN 1345-3041
Volume Number 87 - September 1999

Contents

http://global.mitsubishielectric.com/pdf/advance/vol87/87tr2.pdf

Ecofriendly Ozone-Based Wet Processes for Electron Device Fabrication

*by Hirozoh Kanegae**

Mitsubishi Electric has developed ozone-based wet processes for fabrication of LCDs and other semiconductor devices. These low-cost and low-environmental-impact processes use tiny amounts of chemical reactants and can be conducted at room temperature. This report introduces technology for contamination-free production of high-density ozone and ozonated water, and discusses use of ozonated water as a substitute for a standard RCA cleaning process and for the removal of photoresist.

Public concern is driving manufacturers to reduce the environmental impact of their manufacturing processes. The imperative to manufacture good products at a low price is in transition to a new model of sustainable development in which consumers and manufacturers jointly participate.

Reducing the environmental impact associated with manufacturing processes is now taking importance alongside the more conventional objectives of making electronic equipment smaller, lighter and more power efficient. Novel manufacturing processes will consume smaller energy, chemical and gas supplies, reducing both cost and manufacturing wastes with small footprint installations.

This article introduces cost-effective and environmentally-friendly wet cleaning processes for semiconductor-device and LCD fabrication using ozonated water. Ozone is a strong oxidizing agent suitable for wafer cleaning and its only breakdown product is oxygen.

Ozone Gas and Ozonated Water

Ozone consists of three oxygen atoms joined by covalent bonds with a strength somewhere between single and double bonds. Its applications include disinfecting and deodorizing drinking water supplies, bleaching and removal of organics in wastewater, and surface treatment and oxidation of organic materials in industrial processes. All of these applications rely on ozone's powerful oxidation capabilities and harmless decomposition to oxygen.

Like other gases, ozone's solubility in water obeys Henry's Law. The amount of ozone that dissolves in water increases as the partial pressure of ozone rises and as the water temperature

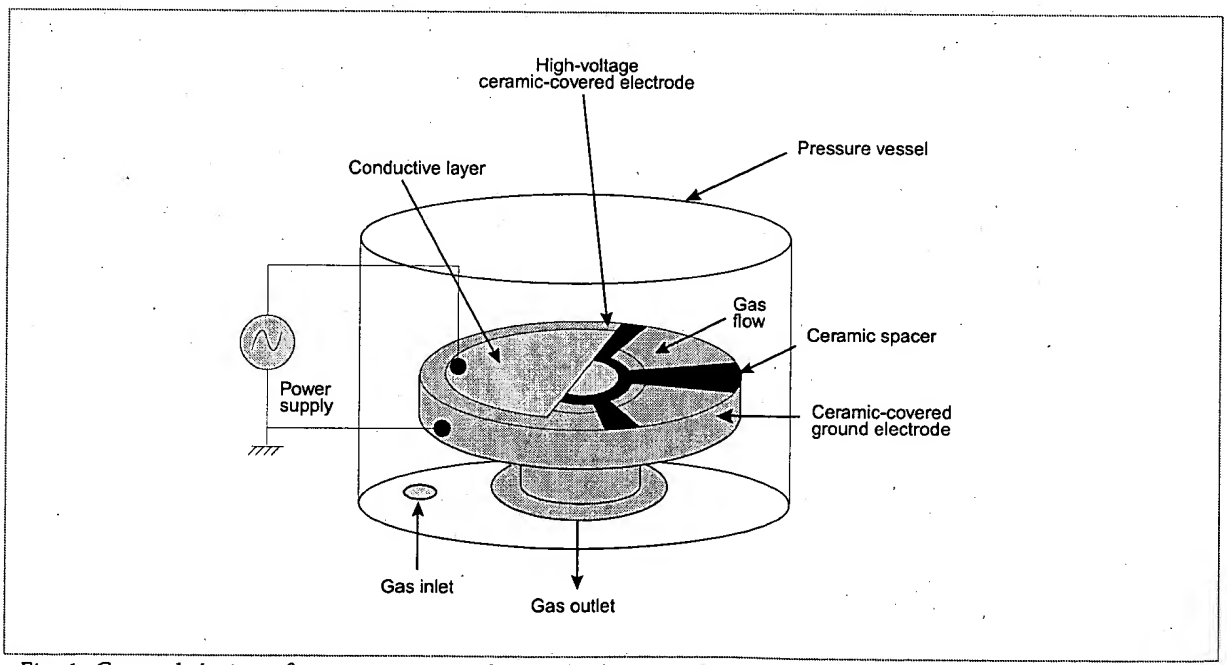

Fig. 1 General design of an ozonizer producing high-concentration contamination-free ozonated oxygen.

**Hirozoh Kanegae is with the Advanced Technology R&D Center.*

drops. The following rule for calculating dissolved ozone concentration is based on experimental measurements.

$$Cw = 0.604(1+t/273)/(1+0.063t)\backslash Cg \quad \text{..... Eq. 1}$$

where Cw is the dissolved ozone concentration in mg/l, Cg is the atmospheric ozone concentration in mg/l, and t is the water temperature in degrees Centigrade.

Ozone has three main mechanisms of chemical activity. First, it attacks the unsaturated bonds in double bonded and aromatic hydrocarbon chains by the well known Criegee mechanism yielding ketones, carboxylic acid and carbon dioxide. Second, it reacts with water to form the hydroperoxy radical (HO_2.) and hydrogen peroxide (H_2O_2) which attack saturated hydrocarbon chains. Third, it reacts with inorganic materials based on the difference in oxidation-reduction potential and oxidizes all metals except gold and platinum.

Controlling Contaminants

To replace the highly evolved manufacturing processes currently used for semiconductor production, ozone based processes will have to achieve comparable tact (or process "step") times and control contaminants that would adversely affect yields. High concentrations are required, and ozone and ozonated water generators must achieve the cleanliness required by today's high scales of integration.

Fig. 1 shows the basics of a system that produces clean, high-concentration ozone. A narrow discharge gap is formed by a conductive layer on the bottom surface of disc-shaped ceramic substrate and a ceramic-coated ground electrode separated by a ceramic spacer. The electrodes are housed in a pressure vessel. Oxygen gas supplied to the vessel passes through the discharge gap and exits through a port in the center of the ground electrode as ozonated oxygen[1],[2]. The discharge gap is extremely narrow to prevent temperature rise of gas in the gap and to control the number of low-energy electrons that could cause the ozone to break down. These features enables the system to

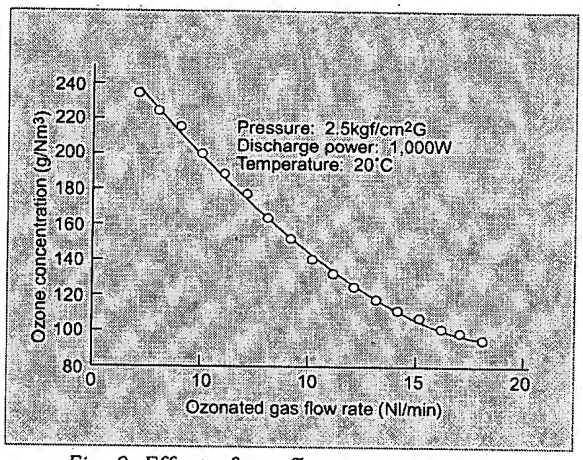

Fig. 2 Effect of gas flow rate on ozone concentration.

achieve ozone concentrations over 230g/Nm³ at a gas flow rate of 2*l*/min (Fig. 2).

In addition to high concentration, ozone produced for semiconductor manufacturing must be free of metallic contaminants. This is achieved by ensuring that the gas contacts only ceramic surfaces. Metallic contamination of the ozonated water was measured at below the parts per trillion detection levels of microwave induced plasma mass spectroscopy and flameless atomic absorption spectroscopy (Table 1).

Wafers immersed in ozonated water were then tested for metallic contamination by total reflection X-ray fluorescence spectroscopy and typical contaminants including Ca, Cr, Mn, Fe, Ni and Cu were below the detection threshold of 1×10^{10} atoms/cm².

A particle counter at the ozone generator's outlet detected no particles over 0.27μm in diameter[3].

Table 1 Metallic Contaminants in Ozonated Water

Element	Na, K, Ca, Fe, Zn, Al	Mg, Ni, Cu	Cr, Mn
Concentration (DI water)	<50ppt	<20ppt	<10ppt
Conc. (ozonated DI water)	<50ppt	<20ppt	<10ppt
Detection threshold	50ppt	20ppt	10ppt

Ozonated Water Cleaning Technology

Control of particles and other contaminants is essential to maintain high yields in production of high-density memory devices. At present, this is accomplished using a series of chemical baths known as the RCA washing method[4]. Initially, a sulfuric acid and hydrogen peroxide bath (SPM) at 120~150°C removes organics and some metallics. Second, a bath of dilute hydrofluoric acid (DHF) at room temperature removes the oxide layer and incorporated metallic contaminants. Third, an ammonium hydroxide and hydrogen peroxide bath (APM) at 80~90°C removes particles. Fourth, an 80~90°C bath of hydrochloric acid and hydrogen peroxide (HPM) removes metals. Finally, dilute hydrofluoric acid is used to remove metallics from the oxide layer formed in the preceding step. Seven rinsings in deionized water follow for a total of 12 process steps (Table 2). LCD manufacture employs a similar process with fewer steps, but the large substrate size means larger baths that consume more chemical supplies.

Replacing these complicated cleaning procedures with ozonated water cleaning dramatically reduces use of chemical supplies, saving the cost of the chemicals and waste processing. Ozone processing also eliminates processing at elevated temperatures, avoiding the associated venting of vapors to the atmosphere. Reduced rinsing saves dionized water.

Ozone can oxidize organic residues from photoresist processes. Spin washing the wafers with ultrasonically activated ozonated water achieves cleaning performance equivalent to a sulfuric acid and hydrogen peroxide bath[5].

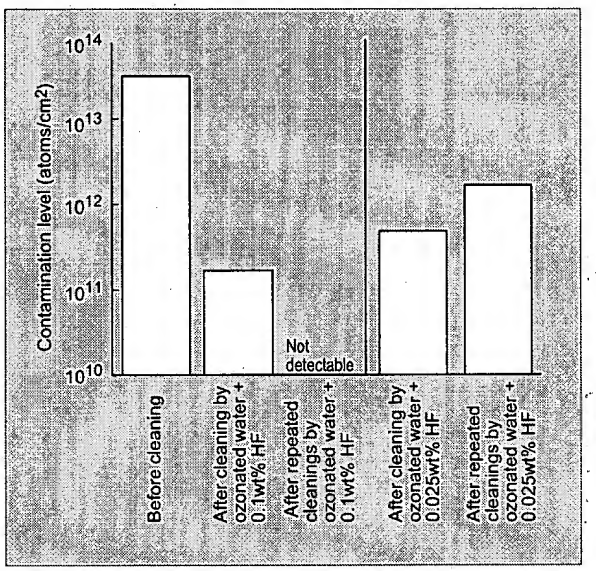

Fig. 3 Copper contamination on wafers before and after cleaning. The ozone concentration is 12ppm.

Ozonated water alone does not remove metallic contaminants incorporated into the oxide layer, but is effective when supplemented by a 0.1% hydrofluoric acid solution, a combination that has been thoroughly investigated[6],[7]. Fig. 3 shows that ozonated water bath with hydrofluoric acid reduces copper contamination with performance comparable to a conventional hydrochloric acid and hydrogen peroxide bath. The acid exposes metallic contaminants embedded in the oxide layer, so that an oxidation reaction can proceed. This forms metal ions that are drawn into solution. This constitutes a dramatic reduction in chemical usage.

Table 2 A Comparison of RCA and Ozonated Cleaning Systems

Method \ Target		Organic photoresist residue	Particles	Metals	Native oxides
RCA cleaning	Cleaning agent	SPM	APM	HPM	DHF
	Mechanism	Oxidative decomposition	Electrical repulsion	Dissolution	Etching
Ozonated water cleaning	Cleaning agent	Ozonated water			
	Mechanism	Oxidative decomposition	Dissolution		
	Acceleration method	Ultrasonic power	pH control and ultrasonic power		Add a little HF

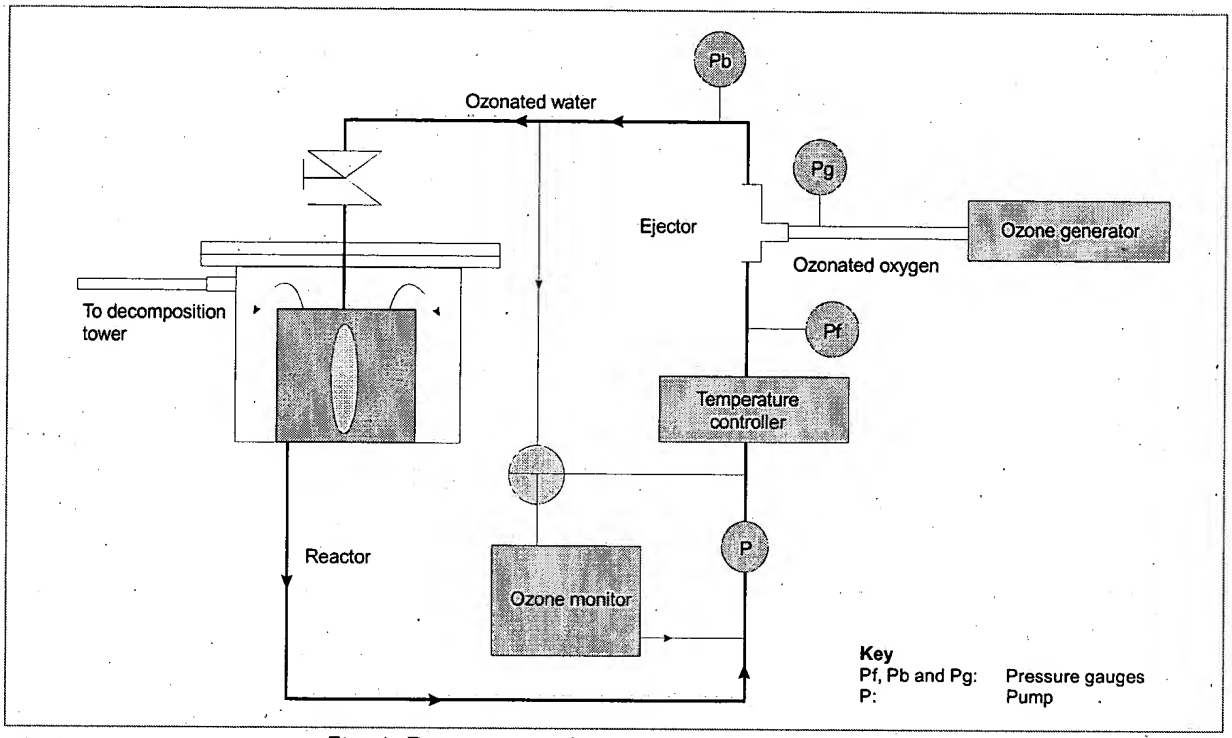

Fig. 4 Resist removal apparatus with ozone ejector

Use of ozonated water for particle removal has been investigated[7],[8]. The ammonium hydroxide and hydrogen peroxide bath normally used has a high pH so that particles receive a negative charge repelling them away from the negatively charged wafer. Since ozone water solutions are either neutral or mildly acidic, ozonated water processes will require activation by pH modifiers or ultrasonic energy. Replacing the ammonium-hydroxide based process eliminates a major source of ammonia contamination, increasing yields and reducing clean air consumption.

Ozonated Water for Photoresist Removal

Photoresists can be removed by oxygen plasma ashing (a dry process), by organic solvents, or in a sulfuric acid and hydrogen peroxide bath. For processing LCD panels, a mixture of dimethyl sulfoxide (DMSO) and monoethanol amine (MEA) is generally used.

Both the solvent and sulfuric acid process are performed at elevated temperature and vent fumes. In the widely used sulfuric acid peroxide process, Caro's acid (H_2SO_5) strips the resist, which oxidizes as soon as it is free. From an environmental impact perspective, trapping the fumes requires special equipment and the bath must be periodically replaced following depletion of the hydrogen peroxide.

An ozone-and-water method would not require the high temperatures or fume traps of the sulfuric acid method, reducing air costs and saving on dionized water—a much smaller environmental impact.

When an ozone concentration of 150~250g/Nm^3 and ozonated water flow of 4.0 *l*/min is used in the ejector-type resist stripping apparatus of Fig. 4, Fig. 5 shows the stripping performance for positive resist. The stripping rate is proportional to the water's ozone concentration and increases with temperature.

Fig. 6 shows the normalized resist removal rate as a function of temperature. R is inversely

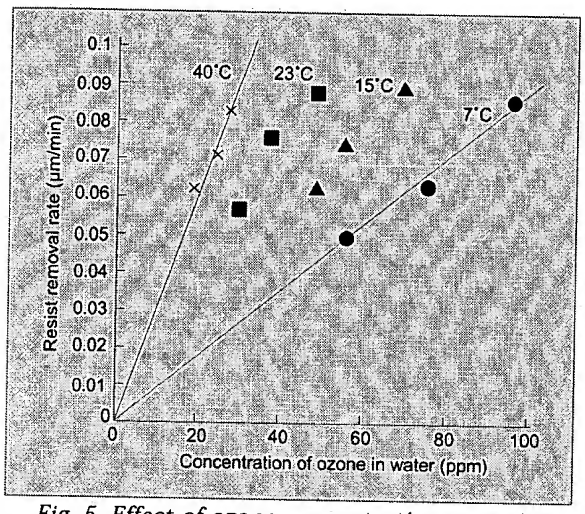

Fig. 5 Effect of ozone concentration on resist removal rate.

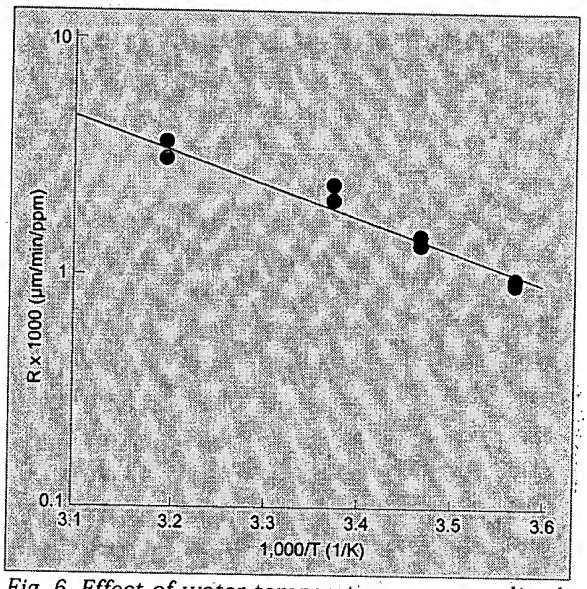

Fig. 6 Effect of water temperature on normalized resist removal rate.

proportional to T, expressed according to Arrehenius' equation:

$$R = R_o exp(-E/kT) \quad \text{..... Eq.2}$$

where R_o is the frequency factor, k is Boltzman's Constant, T is the water temperature (K) and E is the activation energy.

The activation energy calculated from Fig. 6 and Eq. 2 is 0.29eV, substantially smaller than the 4~5eV activation energy needed for carbon-to-carbon single and double bonds or carbon-to-oxygen single bonds, suggesting that one or more intermediate steps are involved[9].

The rate of reaction increases with temperature, but the dissolved ozone capacity reduces with temperature according to Eq. 1. For maximum resist removal speed, the processing temperature should be set to a level that matches the activation energy requirements of the resist. The type of resist, degree of baking, and the presence of ion implantation all affect activation energy. A key issue in ozone-based resist removal systems is achieving satisfactory removal speed.

Chemical-free, energy-saving room-temperature ozone-based processes promise to reduce the cost and environmental impact of semiconductor and LCD manufacture. Development of an efficient silent discharge ozone generator capable of supplying a high concentration of clean ozonated oxygen and a clean ozonated water generator promises to revolutionize semiconductor wafer and LCD cleaning and resist removal. ❑

References

1. Details are available, in Japanese only, in *Mitsubishi Denki Giho*, Vol.73 No.5 (May 1999).
2. J. Kitayama, M. Kuzumoto: Theoretical and Experimental Study on Ozone Generation Characteristics of an Oxygen-fed Ozone Generator in Silent Discharge, J.Phys.D, 30, 2453-2461 (1997)
3. Details are available, in Japanese only, in *Mitsubishi Denki Giho*, Vol.73 No.5 (May 1999).
4. W. Kern, D. Puotinen: Cleaning Solution based on Hydrogen Peroxide for use in Silicon Semiconductor Technology, *RCA Review*, 31, 187 (1970).
5. S. Ojima, K. Kubo, M. Toda, T. Ohmi, Megasonic Excited Ozonized Water for the Cleaning of Silicon Surfaces, J. Electrochem. Soc., 144, 1482 (1997).
6. Details are available, in Japanese only, in *Mitsubishi Denki Giho*, Vol.73 No.5 (May 1999).
7. T. Osaka, A. Okamoto, K. Saga, H. Kuniyasu, T. Hattori, Environment Friendly Single Water Spin Cleaning with Alternate Use of Ozonated Water and Dilute HF, 7th Intl. Symp. on Semiconductor Manufacturing, pp.113 (1998).
8. M. Alessandri, E. Bellandi, B. Crirelli, F. Pipia, K. Wolke, M. Schenkl: Particle Removal Efficiency and Silicon Roughness in HF-DIW/O_3/Megasonics Cleaning, USPSS '98, pp.13 (1998).
9. Details are available, in Japanese only, in *Mitsubishi Denki Giho*, Vol.73 No.5 (May 1999).

The mechanism of anisotropic, electrochemical silic etching in alkaline solutions

Seidel, H.
Messerschmitt-Bolkow-Blohm GmbH, Muenchen, West Germany;

This paper appears in: **Solid-State Sensor and Actuator Workshop, 1990 Technical Digest., IEEE**

Meeting Date: 06/04/1990 - 06/07/1990
Publication Date: 4-7 June 1990
Location: Hilton Head Island, SC USA
On page(s): 86 - 91
Reference Cited: 23
Inspec Accession Number: 3897830

Abstract:
Some experimental data on the anisotropy, selectivity, and voltage dependen anisotropic silicon etchants are given. An attempt is undertaken to provide a unifying model describing the reaction mechanism and the key features of all anisotropic etchants of silicon. It is shown that the reaction is electrochemical comprising the transfer of four electrons between the electrolyte and the solic dissolution of one silicon atom. The crystallographic anisotropy can be attribu differences of the binding energy of surface atoms depending on their respect orientations. High boron concentrations induce the shrinking of a space charg the silicon surface, which in turn leads to the fast recombination of electrons i the conduction band making them no longer available for the reduction of wat electrochemical etch stop at positive potentials is due to the anodic oxidation The finite etch rate observed at etch stop potentials was found to correspond etch rate of SiO_2

Index Terms:
electrochemistry electron-hole recombination elemental semiconductors etching sili alkaline anisotropic etchants anisotropy anodic oxidation binding energy conductior electrochemical reaction electrolyte etch rate etch stop reaction mechanism recon selectivity space charge layer surface orientations unifying model

Documents that cite this document
There are no citing documents available in IEEE Xplore at this time.

THE MECHANISM OF ANISOTROPIC, ELECTROCHEMICAL SILICON ETCHING IN ALKALINE SOLUTIONS

H. Seidel

Messerschmitt-Bölkow-Blohm GmbH, P.O. Box 801109,
8000 München 80, Federal Republic of Germany

ABSTRACT

In this paper, some experimental data on the anisotropy, selectivity, and voltage dependence of anisotropic silicon etchants are given. Furthermore, an attempt is undertaken to provide a general unifying model describing the reaction mechanism and the key features of all alkaline anisotropic etchants of silicon. It is shown that the reaction is electrochemical, comprising the transfer of four electrons between the electrolyte and the solid for the dissolution of one silicon atom. The crystallographic anisotropy can be attributed to small differences of the binding energy of surface atoms depending on their respective surface orientation. High boron concentrations induce the shrinking of a space charge layer on the silicon surface, which in turn leads to the fast recombination of electrons injected into the conduction band making them no longer available for the reduction of water. The electrochemical etch stop at positive potentials is due to the anodic oxidation of silicon. The finite etch rate observed at etch stop potentials was found to correspond well to the etch rate of SiO_2.

INTRODUCTION

Anisotropic silicon etching is a key technology for the fabrication of micromechanical devices. It allows for the precise three-dimensional structuring of miniature sensors and actuators in an IC compatible way. The three main properties that make this technique so widely applicable are the dependence of the etch rate on crystal direction, dopant concentration and on an applied electric potential. The crystallographic anisotropy provides the possibility for a very precise lateral machining of a device by proper alignment of structural contours with either fast or slow etching crystal planes. The dependence on dopant concentration and on electric potential allow for the incorporation of well defined etch stop layers by either using a high boron concentration [1,2], or else exploiting the potential drop across a pn junction [3,4].

Any alkaline solution of sufficiently high pH value (larger than 12) is known to exhibit the same key features listed above. That includes purely inorganic aqueous solutions of KOH, NaOH, LiOH, CsOH, and NH_4OH, with the possible addition of an alcohol [5-7], as well as organic aqueous solutions containing ethylenediamine [8,9], hydrazine [10,11], or choline [12], where additives like pyrocatechol and pyrazine can be present.

The main differences among these etchants are their degree of selectivity with respect to boron doped layers, the etch rate ratio of silicon to silicon dioxide, the influence of diffusion effects which is related to the obtainable surface morphology, as well as the tendency for residue formation.

So far, several papers have been published providing experimental data and models for describing specific aspects of the etching mechanism [8,13-20]. In this article, an attempt is undertaken to provide a general unifying model for all alkaline anisotropic silicon etchants, explaining the key features listed above.

EXPERIMENTAL RESULTS

Anisotropy

The central feature of all anisotropic etchants is the slow etch rate of the (111) crystal planes, being approximately one to two orders of magnitude smaller than for other principal crystal orientations. As an example the silicon etch rates of the three principal crystal orientations obtained in an ethylenediamine based solution (EDP type S) are shown in Fig. 1. This diagram also shows, that the activation energies are smaller for fast etching crystal planes and vice versa. This effect has been observed for other anisotropic etchants, as well [18]. Therefore, the anisotropy ratio generally decreases with rising temperature.

Influence of dopants

For boron concentrations above a critical value C_0 of approximately $3*10^{19}$ cm^{-3} a drastic reduction of the etch rate can be observed on both <100> and <110> wafers. This effect is shown in Fig. 2 for an EDP solution type S, where the absolute etch rate was normalized by the etch rate for moderately doped silicon. The drop is inversely proportional to the fourth power of the boron concentration.

When using KOH solutions, very similar results to EDP are obtained for low concentrations up to 10 %. However, the relative etch stop effect becomes smaller when increasing the concentration of the solution.

For comparison, results obtained for germanium doped epitaxial silicon layers and for phosphorous doped layers have been included in Fig. 2. Even at very high germanium concentrations of $1*10^{21}$ cm^{-3} only a relatively small

CH2783-9/90/0000-0086$01.00©1990 IEEE

reduction of the etch rate can be observed. Similarly, the reduction of the etch rate obtained for phosphorus doped layers, as published by Palik et al. [13], is relatively small.

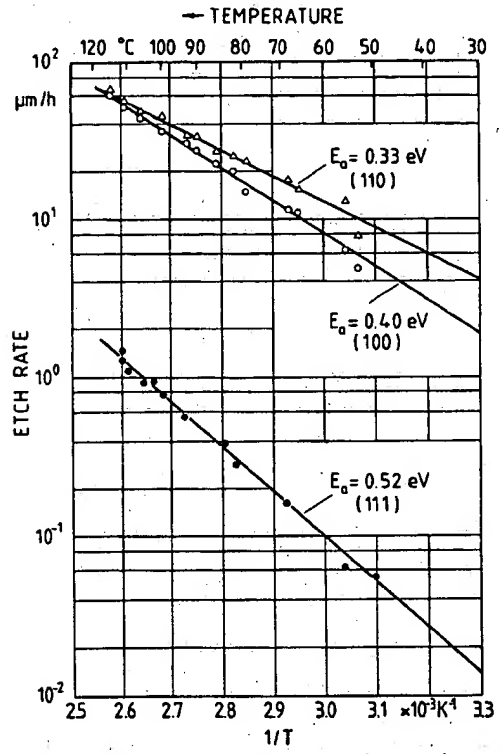

Fig. 1: Arrhenius diagram of the etch rates for the three main crystal planes, when using an EDP solution type S of the following composition: 1 l ethylenediamine, 133 ml water, 160 g pyrocatechol, and 6 g pyrazine.

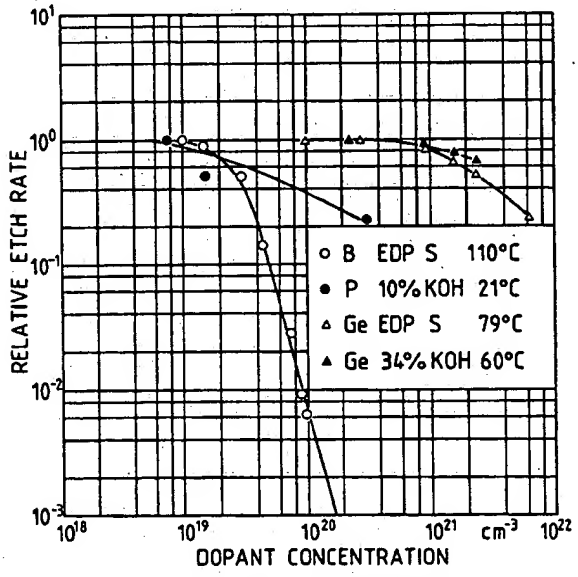

Fig. 2. Normalized etch rates for silicon layers doped with boron, phosphorus [13], and germanium, respectively.

Electrochemical etching

When applying an external potential to a silicon wafer during the etching process, the etch rate can be influenced drastically. This is shown in Figs. 3 and 4 for p and n type silicon, respectively. Correlated voltammograms are also included in these diagrams. At anodic potentials the current density rises up to a certain point and then suddenly drops very sharply to a drastically reduced value, which is a behavior typical for the formation of a passivation layer. At this passivation potential a drastic drop of the etch rate can also be observed. The highest etch rate is obtained at a point slightly anodic from the open circuit potential (OCP). At cathodic potentials, the etch rate decreases gradually.

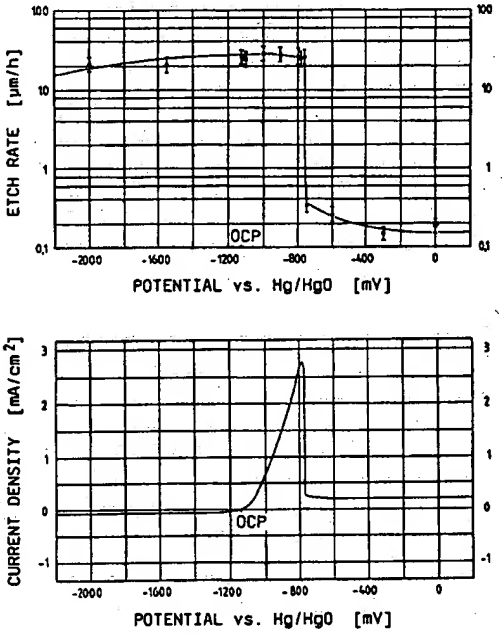

Fig. 3. Correlation between the voltammogram and the etch rate of p-type silicon in a 30 % KOH solution at a temperature of 65 °C. Potential is relative to a Hg/HgO reference electrode.

Whereas the etch rates obtained for n and p type silicon are very much the same, the currents flowing for cathodic potentials differ very much. P type silicon behaves like a backward biased diode for negative potentials, whereas n type silicon exhibits a large current similar to a forward biased diode.

The temperature dependence of the etch rate of n type silicon for three different potentials is shown in the Arrhenius diagram in Fig. 5. At the open circuit potential of about - 1.1 V the activation energy is 0.62 eV, which is in good agreement with previously observed values [18]. At a cathodic potential of - 2 V, the etch rate is somewhat lower with a slightly decreased activation energy. A drastically reduced etch rate can be observed for an anodic potential of 0 V. For comparison, a

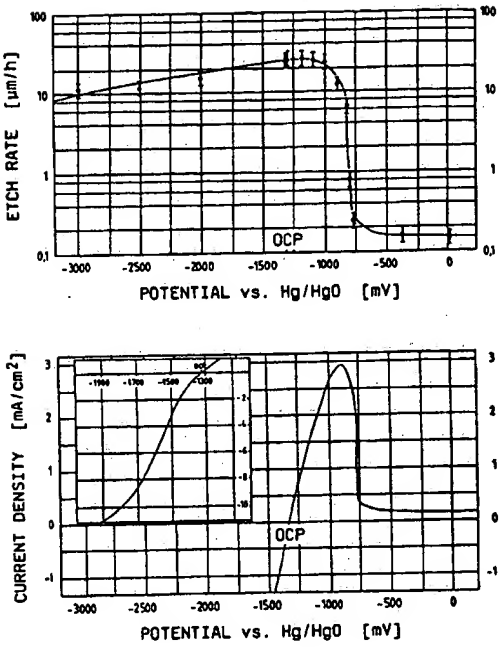

Fig. 4. Correlation between the voltammogram and the etch rate of n-type silicon in a 30 % KOH solution at a temperature of 65 °C.

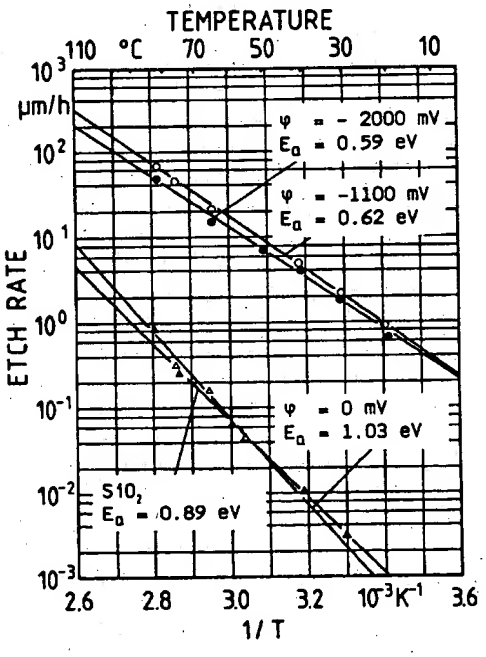

Fig. 5. Arrhenius diagram of the silicon etch rates obtained in a 30 % KOH solution for three different potentials. For comparison, the etch rate curve of silicon dioxide has been included.

curve for the etch rate of silicon dioxide has been included. Both the etch rate and the activation energy are found to be in good agreement. This is a strong indication, that the passivation layer that forms is silcon dioxide.

DISCUSSION

In the following an electrochemical model for the etching mechanism is proposed, which is considered to be valid for all alkaline silicon etchants. The model will first be described for moderately doped silicon with (100) orientation. Then the modifications arising for other crystal orientations and for high dopant concentrations, as well as when applying an external potential will be discussed.

Reaction mechanism

From the experimental results described above and from Raman spectroscopy measurements performed by Palik et al. [14] it can be concluded, that hydroxide ions and water are the main reactants on the side of the electrolyte. Therefore, the redox couple H_2O/OH^- is assumed to play a key role in the reaction. The Fermi level of this redox couple is initially higher than that of silicon, leading to a transfer of electrons into the solid after immersion into the electrolyte [18]. Thereby, a space charge layer is formed on the silicon surface, which corresponds to a downward bending of the energy bands. This situation is shown in Fig. 6.

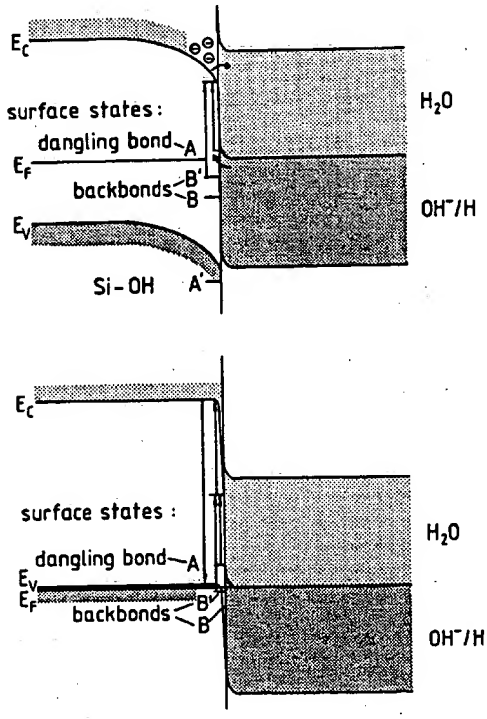

Fig. 6. Energy bands of moderately p doped silicon and the H2O/OH- redox couple. Surface states A and B in silicon correspond to dangling bonds and backbonds, respectively.

Due to the different bonding situation of atoms located near the surface of the silicon crystal, surface states arise which are located within the forbidden bandgap. In our model, two types of surface states are considered to be important. Type A, which is indicated in Fig. 6 is correlated to the dangling bonds. Type B with a lower energy level corresponds to the backward directed binding electrons of the surface atoms to the second layer of atoms, so-called backbonds.

In a first step, two hydroxide ions bind to the two dangling bonds available for a (100) surface silicon atom. They inject two electrons into surface state A, which are then lifted into the conduction band by thermal excitation:

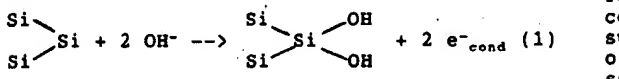

Due to the presence of the bonded hydroxide groups on the crystal surface, the strength of the backbonds of the surface atoms will be reduced, leading to a shifting of the energy level of surface state B to a somewhat higher value.

In the next step, the backbonds of the $Si(OH)_2$ groups are broken by thermally lifting the corresponding surface state electrons (B) into the conduction band. Thus, a positively charged silicon-hydroxide complex is formed, which is detached from the lattice, but still attracted by electrostatic forces:

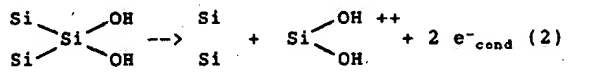

We assume that the energy difference between the surface state and the conduction band correlates to the measured activation energy in KOH solutions, being approximately 0.6 eV. Thus, this step can be considered to be rate limiting for the total reaction. The smaller activation energy of 0.40 eV for the same crystal plane obtained for an EDP solution can be attributed to the larger influence of diffusion effects due to the smaller pH value.

The silicon hydroxide complex reacts further with two more hydroxide ions producing orthosilicic acid [21]:

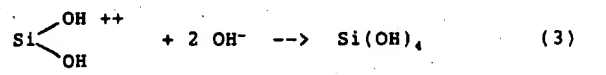

It can be assumed, that the breaking of the backbonds described by eqn. (2) and the bonding of hydroxide ions according to eqn. (3) happen more or less simultaneously. When the $Si(OH)_4$ molecule reaches the bulk electrolyte by diffusion, it will not stay stable. It is well known in silicate chemistry, that for pH values exceeding 12 the following complex will be formed by the separation of two protons [21], which was observed by Raman spectroscopy measurements [14]:

$$Si(OH)_4 \rightarrow SiO_2(OH)_2^{--} + 2\ H^+ \qquad (4)$$

The excess electrons in the conduction band react with water molecules situated at the silicon surface, producing hydroxide ions and hydrogen atoms:

$$4\ H_2O + 4\ e^- \rightarrow 4\ OH^- + 2\ H_2 \qquad (5)$$

In the energy diagram shown in Fig. 6, this step corresponds to the transfer of conduction band electrons localized near the silicon surface into the unoccupied state of the H_2O/OH^- redox couple, as indicated by the arrow. Therefore it is required, that an overlap between the conduction band and the upper state of the redox couple exists.

The four hydroxide ions consumed in the oxidation step are assumed to be generated by the reduction of water (eqn. (5)), rather than coming from the bulk electrolyte. This view is supported by the relatively small difference of the silicon etch rates between EDP and KOH solutions, although the concentration of hydroxide ions differs by a factor of more than 100. Furthermore, for large KOH concentrations the etch rate decreases with the fourth power of the water concentration [18].

The overall gross reaction is summarized as follows:

$$Si + 2\ OH^- + 2\ H_2O \rightarrow SiO_2(OH)_2^{--} + 2\ H_2 \qquad (6)$$

The formation of residues on the silicon surface is most severe for solutions with a relatively high water concentration. In this case the silicon dissolution rate is so high, that the transfer of the $Si(OH)_4$ complex away from the surface cannot keep up with its production. Thus, a polymerization by the separation of water leads to the formation of an SiO_2-like complex, which was actually observed by Wu et al. [22].

Anisotropy

The central feature of the anisotropic behavior of silicon etchants is the very low etch rate of (111) planes. (111) surface atoms possess only one dangling bond, whereas there are two for all other main crystal surfaces. Thus in the initial reaction corresponding to eqn. (1), only one hydroxide can bind to a surface atom. Subsequently, three backbonds have to be broken in analogy to eqn. (2). This reaction step requires the transfer of the respective binding electrons into the conduction band by thermal excitation. The energy level of the corresponding surface state B must be lower than for a (100) surface. We assume, that this energy difference corresponds roughly to the observed differences in activation energy between (100) and (111) surfaces of approximately 0.12 eV (compare Fig. 1).

Influence of dopants

For very high boron dopant concentrations, the silicon etch rate was found to decrease inversely proportional to the fourth power of the boron concentration. The critical boron concentration above which this decrease actually starts coincides well with the published value of $2.2*10^{19}$ cm^{-3} for the onset of degeneracy [23]. For a degenerate p type semiconductor the Fermi level drops into the va-

lence band which is indicated in Fig. 6. As a consequence, the width of the space charge layer shrinks to a very small value on the order of one atomic layer, which is comparable to the situation observed on a metal electrode. Thus, the potential well given by the downward bending of the energy bands on the silicon surface becomes very small and, therefore, can no more confine the electrons injected into the conduction band by the oxidation step (eqns. (1) and (2)).

These injected electrons will therefore be forced to penetrate through the surface charge layer into deeper regions of the crystal. Due to the very large hole concentration, they will have a high probability to recombine with a hole from the valence band. As a consequence, these injected electrons are no more available for a subsequent reduction step, which is required for the generation of new hydroxide ions at the silicon surface (eqn. (5)).

The remaining etch rate observed for high boron concentrations is determined by the number of available electrons in the conduction band at the silicon surface. Under equilibrium conditions, this number is inversely proportional to the number of holes (np = const.), i.e. to the boron concentration. We assume that this inverse proportionality is also valid at the crystal surface. Since four electrons are required for the dissolution of one silicon atom, the fourth power dependence of the etch rate on the boron concentration can be explained.

Influence of electric potential

The key feature is the drastic reduction of the etch rate on both p and n type silicon electrodes for anodic potentials of approximately 0.5 V. The observed residual etch rate and its activation energy proofed to coincide well with the values for a silicon dioxide layer, as indicated in Fig. 5. Therefore, we assume that an SiO_2 passivation layer forms by the anodic oxidation of silicon, which was already suggested by several other authors [4,16]. Starting from the result of eqn. (3), this process can be described by the following reaction:

$$Si(OH)_4 \dashrightarrow SiO_2 + 2\ H_2O \qquad (7)$$

This oxide layer is assumed to start growing, as soon as the negative surface charge on the silicon electrode is cancelled by the externally applied positive potential. This corresponds to the flat band situation. Starting from this potential, hydroxide ions from the bulk of the solution are no more repelled and can easily approach the silicon surface in very large numbers. As soon as the oxide layer starts growing, the reduction of water according to eqn. (5) can no longer take place and the generation of hydroxide ions and free hydrogen at the surface stops. Interestingly, the measured current density at etch stop potential is well correlated to the silicon dissolution rate, according to the sum of eqns. (1-3) (compare with Figs. 3 and 4). This is a further proof for the transfer of four electrons required for the dissolution of one silicon atom.

The small increase of the etch rate at potentials slightly positive from open circuit conditions and, similarly, the gradual decrease of the etch rate at cathodic potentials indicates, that the electrostatic force on the OH^- ions has an influence on their availability at the silicon surface. This view is supported by the observation that cathodically etched surfaces show typical signs of diffusion effects, like the formation of deeper trenches along the periphery of an etch cavity.

CONCLUSIONS

The two key parameters for the etching behavior of alkaline solutions on silicon and on passivation layers are the molar water concentration and the pH value, which is a measure of the concentration of hydroxide ions. Anions do not play a significant role in the reaction. These effects are summarized in Tab. 1.

	- H_2O +	- pH +
SiO_2 etch rate	no effect	- ⟵ +
Si etch rate	- ⟶ +	little effect
Solubility	no effect	- ⟶ +
Si/SiO_2 ratio	- ⟶ +	+ ⟵ -
Diffusion effects	- ⟶ +	+ ⟵ -
Residue formation	- ⟶ +	+ ⟵ -
p^+ etch stop	- ⟶ +	+ ⟵ -
pn etch stop	- ⟶ +	+ ⟵ -

Tab. 1: Effects of water concentration and pH value on the characteristics of anisotropic silicon etchants.

The importance of organic etchants like of ethylenediamine or hydrazine based solutions does not derive from their complex anions, but rather from the possibility to adjust the pH value and the molar water concentration of water almost independently from each other. This is not the case in KOH solutions and related etchants. The only possibility to influence the water concentration there is by diluting with an alcohol.

ACKNOWLEDGEMENT

The author would like to thank L. Csepregi, H. Baumgärtel, R. Voß, G. Müller, and A. Heuberger for many discussions on the subject, as well as R. Kolbeck and U. Thumser for their help in performing the experiments and preparing the manuscript.

REFERENCES

[1] A. Bohg, "Ethylene Diamine-Pyrocatechol-Water Mixture Shows Etching Anomaly in Boron-Doped Silicon," J. Electrochem. Soc., 118 (1971) 401-402.

[2] H. Seidel and L. Csepregi, "Studies on The Anisotropy and Selectivity of Etchants Used for The Fabrication of Stress-free Structures," Electrochem. Soc. Ext. Abstr., No. 123, p. 194, Montreal, Canada, May 9-14, 1982.

[3] H.A. Waggener, "Electrochemically Controlled Thinning of Silicon," Bell System Tech. J., 50 (1970) 473-475.

[4] B. Kloeck and N.F. de Rooij, "A Novel Four Electrode Electrochemical Etch-Stop Method for Silicon Membrane Formation," in: Proc. 4th International Conference On Solid-State Sensors And Actuators - Transducers '87, Tokyo, Japan, June 2-5, 1987, pp. 116-119.

[5] J.B. Price, "Anisotropic Etching of Silicon with KOH-H2O-Isopropyl Alcohol," in: H.R. Huff and R.R. Burgess (Eds.), Semiconductor Silicon, Electrochemical Society Softbound Proceedings Series, Princeton, NJ, USA, 1973, pp. 339-353.

[6] L.D. Clark Jr., J.L. Lund, and D.J. Edell, "Cesium Hydroxide (CsOH): A Useful Etchant for Micromachining Silicon," in: Technical Digest, IEEE Solid-State Sensor And Actuator Workshop, Hilton Head Island, S.C., USA, June 6-9, 1988, pp 5-8.

[7] W. Kern, "Chemical Etching of Silicon, Germanium, Gallium Arsenide, and Gallium Phosphide," RCA Review, 39 (1978) 278-308.

[8] R.M Finne and D.L. Klein, "A Water-Amine-Complexing Agent System For Etching Silicon," J. Electrochem. Soc., 114 (1967) 965-970.

[9] A. Reisman, M. Berkenblit, S.A. Chan, F.B. Kaufman, and D.C. Green, "The Controlled Etching of Silicon in Catalyzed Ethylenediamine-Pyrocatechol-Water Solutions," J. Electrochem. Soc., 126 (1979) 1406-1415.

[10] M.J. Declercq, L. Gerzberg, and J.D. Meindl, "Optimization of the Hydrazine-Water Solution for Anisotropic Etching of Silicon in Integrated Circuit Technology," J. Electrochem. Soc., 122 (1975) 545-552.

[11] M. Mehregany and S.D. Senturia, "Anisotropic Etching of Silicon in Hydrazine," Sensors and Actuators, 13 (1988) 375-390.

[12] M. Asano, T. Cho, and H. Muraoka, "Application Of Choline In Semiconductor Technology," Electrochem. Soc. Ext. Abstr., No. 354, p. 911, 1976.

[13] E.D. Palik, J.W. Faust, H.F. Gray, and R.F. Greene, "Study of the Etch-Stop Mechanism in Silicon," J. Electrochem. Soc., 129 (1982) 2051-2059.

[14] E.D. Palik, H.F. Gray, and P.B. Klein, "A Raman Study Of Etching Silicon In Aqueous KOH," J. Electrochem. Soc., 130, (1983) 956-959.

[15] N.F. Raley, Y. Sugiyama, and T. van Duzer, "(100) Silicon Etch-Rate Dependence on Boron Concentration in Ethylenediamine-Pyrocatechol-Water Solutions, J. Electrochem. Soc., 131 (1984) 161-171.

[16] O.J. Glembocki, R.E. Stahlbush, and M. Tomkiewicz, "Bias-Dependent Etching of Silicon in Aqueous KOH," J. Electrochem. Soc., 132 (1985) 145-151.

[17] H. Seidel, "The Mechanism of Anisotropic Silicon Etching and its Relevance for Micromachining," in: Proc. 4th International Conference On Solid-State Sensors And Actuators - Transducers '87, Tokyo, Japan, June 2-5, 1987, pp. 120-125.

[18] H. Seidel, L. Csepregi, A. Heuberger, and H. Baumgärtel, "Anisotropic Etching of Crystalline Silicon in Alkaline Solutions - I. Orientation Dependence and Behavior of Passivation Layers," to be published in J. Electrochem. Soc.

[19] H. Seidel, L. Csepregi, A. Heuberger, and H. Baumgärtel, "Anisotropic Etching of Crystalline Silicon in Alkaline Solutions - II. Dopant Concentration Dependence," to be published in J. Electrochem. Soc.

[20] R. Voß, H. Seidel, and R.J. Behm, "Investigations on the Electrochemically Controlled Anisotropic Etching of Silicon in Aqueous KOH," Abstract of The Electrochemical Society European Workshop On Electrochemical Processing Of Semiconductors, Berlin, Germany, April 4-7, 1989, (full length paper to be published in J. Electrochem. Soc.).

[21] R.K. Iler, The Chemistry Of Silica, John Wiley, New York, 1979.

[22] X. Wu, Q. Wu, and W.H. Ko, "A Study on Deep Etching of Silicon Using EPW," in: Digest Of Technical Papers, The Third International Conference On Solid-State Sensors And Actuators, Philadelphia, USA, June 11-14, 1985, pp. 291-294.

[23] A.A. Vol'fson and V.K. Subashiev, "Fundamental Absorption Edge of Silicon Heavily Doped with Donor or Acceptor Impurities," Sov. Phys. Semiconductors, 1 (1967) 327-332.